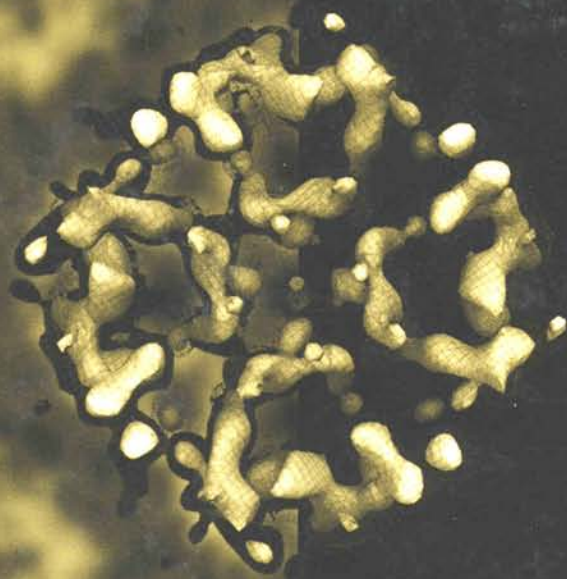


*MOLECULAR BIOLOGY AND PHYSIOLOGY
OF WATER AND SOLUTE TRANSPORT*



Edited by Stefan Hohmann and Søren Nielsen

1.2 Structure function analysis

GLPF: A STRUCTURAL VARIANT OF THE AQUAPORIN TETRAMER

The GlpF projection at 3.5 Å

¹Thomas Braun, ²Ansgar Philippsen, ¹Sabine Wirtz, ³Mario J. Borgnia, ³Peter Agre, ⁴Werner Kühlbrandt, ¹Andreas Engel and ¹Henning Stahlberg

¹M. E. Müller Institute for Microscopy, Biozentrum, University of Basel, Klingelbergstrasse 70, CH-4056 Basel, Switzerland. ²Department of Structural Biology, Biozentrum, University of Basel, Klingelbergstrasse 70, CH-4056 Basel, Switzerland. ³Department of Biological Chemistry, Johns Hopkins University School of Medicine, Baltimore, MD 21205, USA. ⁴Max-Planck-Institute for Biophysics, Kennedyallee 70, D-60596 Frankfurt, Germany. E-mail: Henning.Stahlberg@unibas.ch

1. INTRODUCTION

The glycerol uptake facilitator of *E. coli* (GlpF) (Boos *et al.*, 1990) is one of the few known diffusion facilitators in the inner membrane of this bacterium. Glycerol diffuses into the cell through GlpF and is phosphorylated by the glycerol kinase (GlpK), which prevents back-diffusion. Besides glycerol transport, the diffusion of polyols and urea derivatives through GlpF have been reported (Maurel *et al.*, 1994), but none of these substrates are transported in a phosphorylated state. In contrast, it remains unclear whether GlpF allows the passage of water.

GlpF is a member of the aquaporin protein super-family (formerly known as the MIP family) which includes water channels (AQPs) and the facilitators of small solutes like glycerol (GLPs) (Heymann and Engel, 2000; Park and Saier, 1996; Reizer *et al.*, 1993). All of these channels are strictly selective for non-ionic compounds. Sequence comparisons have revealed an internal homology between the C- and N-terminal halves of all aquaporins, with highly conserved regions in the cytoplasmic loop B and the extracellular loop E (Heymann and Engel, 2000). According to the model of

Molecular Biology and Physiology of Water and Solute Transport.

Edited by Hohmann and Nielsen, Kluwer Academic/Plenum Publishers, New York, 2000.

Jung *et al.* (1994), these two loops fold back into the membrane to form a channel akin to an hourglass. This region is believed to be the site of solute selectivity. A comparison between AQP0 (AQP subcluster) and GlpF (GLP subcluster) is given in Figure 1. Loop E and C of GlpF contain additional amino acids compared to AQP1 and MIP0. Other conserved residues have been found in the aquaporin super-family by (Froger *et al.*, 1998) and demonstrated by (Lagree *et al.*, 1999) to discriminate AQPs from GLPs. In addition (Heymann and Engel, 2000) have identified a pair of residues in helix VI that may determine the size of the pore. Note that all important differences are located at the extracellular surface.

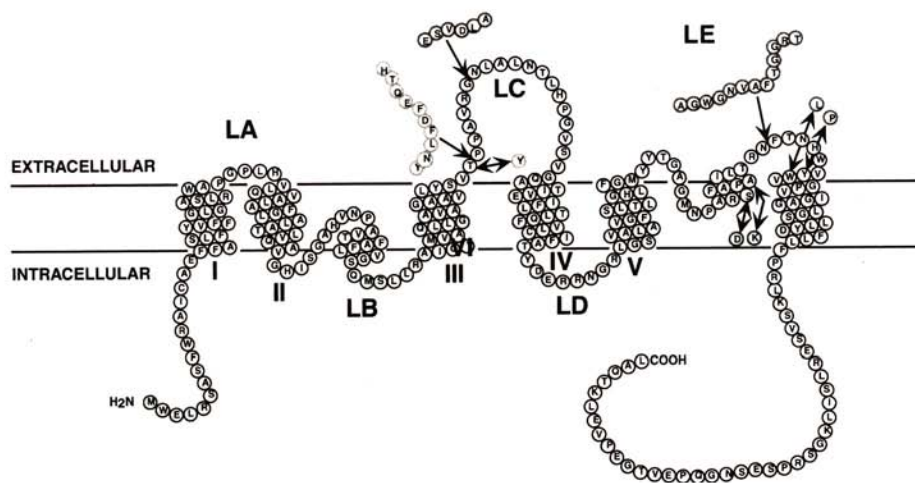


Figure 1. Sequence comparison between the AQP subcluster and the GLP subcluster. Most important differences of GLPs (in this case GlpF from *E. Coli*) are indicated with bold outlines. The reference sequence is AQP0 from the AQP subcluster. Single arrowheaded lines are indicating inserts, double headed lines are indicating aminoacids substitutions. Taken from Froger *et al.* (1998), Heymann and Engel (2000) and Mulders *et al.* (1995).

2. RESULTS

2.1 Protein expression and single particle analysis

GlpF carrying ten C-terminal histidine residues was overexpressed in *E. coli*, solubilized and purified in octyl- β -D-glucopyranoside (OG) as described in (Borgnia *et al.*, 1999). Analysis of purified and solubilized GlpF in SDS-PAGE revealed a prominent band at an apparent molecular weight of 30 kDa. Negatively stained preparations of the solubilized, purified GlpF

were imaged with a transmission electron microscope (TEM). *Figure* shows the homogeneous size distribution of the purified protein that often exhibited a square shape. Occasionally larger complexes can be seen (arrows). Single particles were windowed and subjected to reference-free alignment, resulting in a square-shaped average projection that had a side-length of about 80 Å (Figure 2, inset). Four weak densities can be distinguished at the periphery of the square.

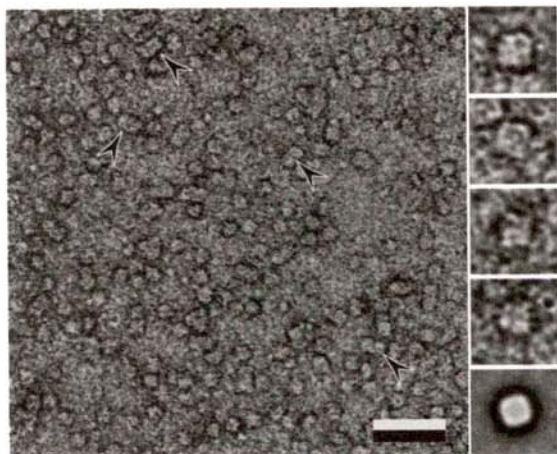


Figure 2. Overview of negatively stained solubilized GlpF in the transmission electron microscope. Square shaped particles are predominant, but complexes of approx. twice the size are also seen (arrows). Scale bar corresponds to 450 Å. Insets: Four selected square-shaped particles and a 4 fold symmetrized average after reference free single particle analysis. Image side length corresponds to 230 Å.

2.2 Two-dimensional crystallization

Solubilized GlpF was reproducibly crystallized using a continuous flow dialyzing device (Jap *et al.*, 1992). A short description of this setup is given in Figure 3. Analysis in the TEM showed polycrystalline vesicles with diameters up to 40 μm and mostly mono-crystalline vesicles with rectangular shapes and diameters up to 8 μm . The crystals diffracted the electron beam beyond 3.3 Å, but weak structure factors between 7 and 5 Å were observed (Braun *et al.*, submitted).

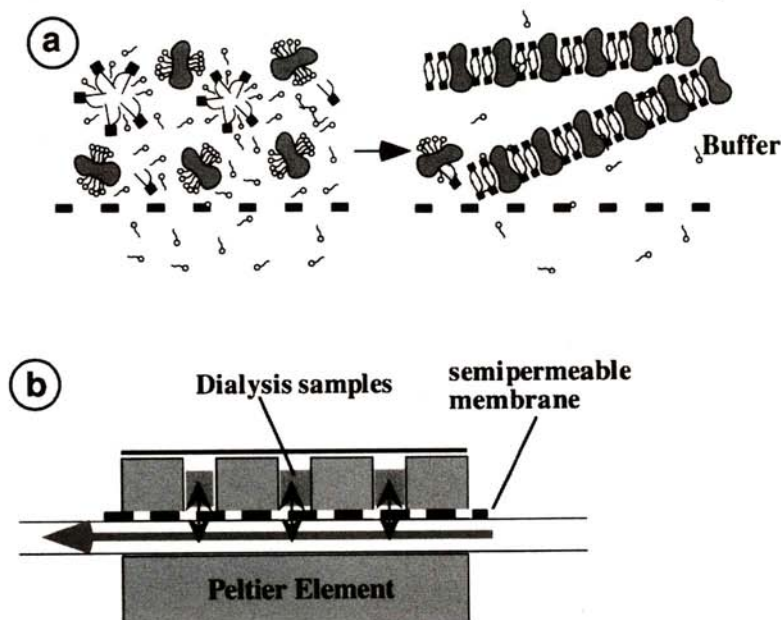


Figure 3 Principle of the used crystallization approach. **a:** Mixed lipid/detergent micelles and solubilized protein is present. Only free detergent can pass the dialysis membrane (dashed line). By dialysing against a buffer without any detergent, the latter is subsequently replaced by lipid in the protein/detergent micelles. Membranes are favoured by the lipids. With the right buffer conditions 2 dimensional crystals are formed. **b:** Principle of a continuous flow dialyzing device as described in Jap *et al.*, (1992). The dialyzing buffer is continuously exchanged. The temperature is controlled by a peltier-element, which allows to run temperature profiles.

2.3 Electron Microscopy and Image treatment

Images of frozen hydrated crystals recorded at low dose revealed sharp spots when examined by optical diffraction out to a resolution of 7 Å. The 9 best images were digitized and processed by the MRC program package (Henderson *et al.*, 1990; Henderson *et al.*, 1986). A general overview over the image processing is given in Figure 4. The phase residuals of the merged data obtained after lattice unbending and transfer function correction indicated significant information up to a resolution of 3.5 Å. The resulting projection map is shown in Figure 5.

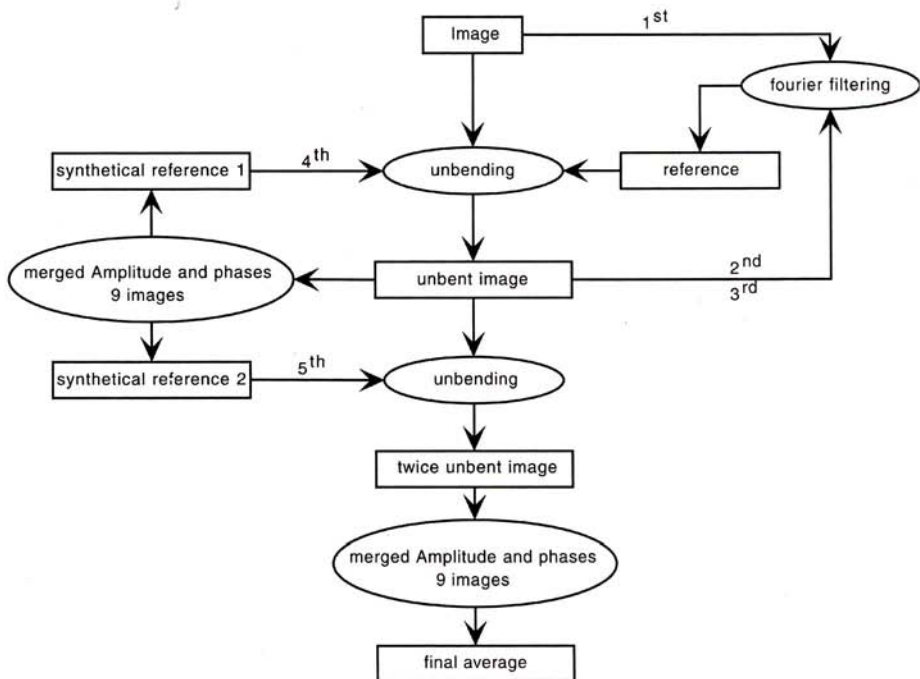


Figure 4. Principle of the applied image processing. In a first run, images were unbent three times, using the Fourier-filtered images themselves as a reference (Henderson *et al.*, 1990; Henderson *et al.*, 1986). The merged amplitudes and phases from 9 images were then used to create a synthetic reference (program MAKETRAN), applying two different negative temperature factors to correct the envelope function. All images were unbent in a fourth run using the reference 1 with the smaller negative temperature factor. The images unbent in this way were then fine-corrected by unbending them again, using the reference 2 with the stronger negative temperature factor, this time allowing only very small (5 pixel/unit-cell) displacements of the unit cells.

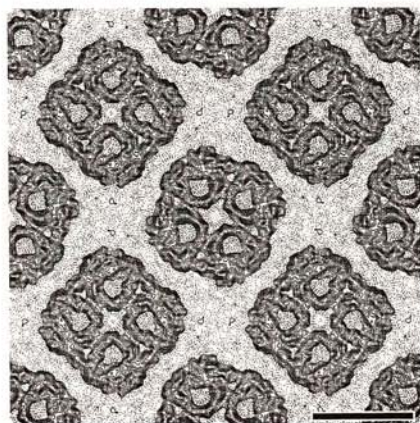


Figure 5. The p4-symmetrized 3.5 Å projection structure of GlpF. The map was calculated by merging 9 electron micrographs after unbending crystal distortions and correcting the transfer function. The phase residuals indicated significant information up to 3.5 Å resolution. Neighboring tetramers are up down oriented as visible in their mirrored handedness. A P4 symmetry was found and not a p42₁2 as in AQP1 (Walz *et al.*, 1994). Unit cell length is 104 Å. A negative temperature factor of -20 \AA^2 was applied. Scale bar corresponds to 50 Å.

3. DISCUSSION

GlpF showed a tetrameric organization throughout the purification. This was monitored by electron microscopy of negatively stained samples taken at various steps and was corroborated by mass-measurements of freeze dried unstained preparations in the STEM (Braun *et al.*, submitted). Thus, GlpF exhibits the same tetrameric structure as other aquaporins previously studied: AQP1 (Smith and Agre, 1991; Walz *et al.*, 1994), AqpZ (Ringler *et al.*, 1999), MIP (Hasler *et al.*, 1998). The tetrameric nature of GlpF supports the model proposed by (Voegelé *et al.*, 1993) that GlpF interacts with the tetrameric glycerol kinase GlpK to stimulate glycerol phosphorylation.

It is interesting to compare the first high-resolution projection structure of the archetypal member of the GLP sub-family with that of AQP1, the first aquaporin structurally analyzed to high resolution (Cheng *et al.*, 1997; Li *et al.*, 1997; Mitsuoka *et al.*, 1999; Walz *et al.*, 1997; Walz *et al.*, 1994) (Figure 6). The density maxima marked in the AQP1 map appear to be slightly shifted in the GlpF map. They are related to the highly tilted helices that surround a central density produced by loops B and E, marked by an X in Figure 6 (Mitsuoka *et al.*, 1999). According to the hourglass model (Jung *et al.*, 1994) this is the site of the channel and differences between GlpF and AQP1 in this region are of particular interest. While the projection map of

AQP1 shows a weak density at this position, GlpF seems to have a much larger hole with no inner structure discernable in the projection map. We may speculate that the weak density seen in the AQP1 channel is related to the phenylalanine in helix VI (Figure 1, Tyrosine in the case of AQP0) found in many water channels. Most GLPs have a leucine at this position (Heymann and Engel, 2000), and indeed, no corresponding density is seen for GlpF.

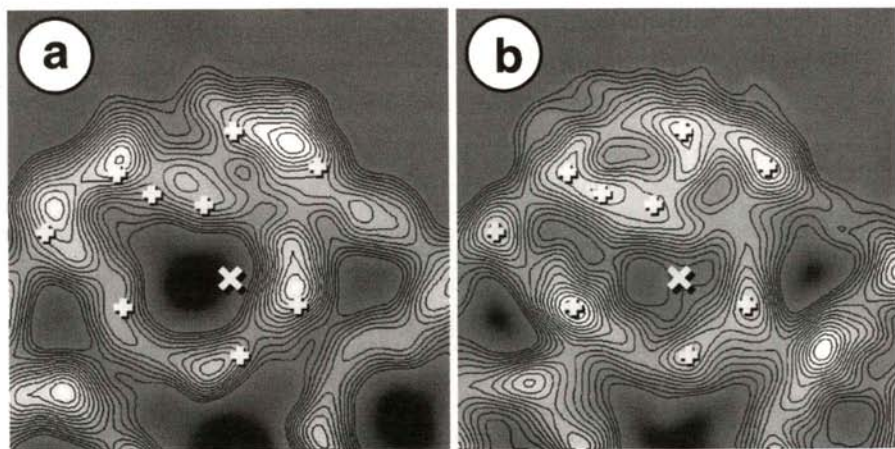


Figure 6. Comparison of GlpF and AQP1 at 4 Å resolution. **a**, GlpF monomer. **b**, AQP1 monomer. Overlaid crosses mark the position of density maxima found in AQP1. The depression in the AQP1 monomer, thought to represent the pore, is marked by an "X". The most prominent difference revealed by the GlpF monomer is the larger central depression of approx. 10 Å diameter. The one in AQP1 has a diameter of roughly 4 Å and a complex shape. Minor differences are seen in the surrounding density maxima. They correspond to the projection of overlapping highly tilted helices. The minima around the four-fold axis and between the monomers are rather similar. The image side length corresponds to 41 Å.

In summary, the projections of GlpF and AQP1 are comparable in their overall architecture but present interesting differences, which may be related to their different biological functions. It is compelling to speculate that the larger depression seen in the GlpF monomer represents the pore where glycerol and similar solutes pass (Maurel *et al.*, 1994). This would in turn support the hourglass model. However, to understand the molecular mechanisms and specificity of water and solute transport in aquaporins, the atomic structures of both AQP1 and GlpF are required. The highly ordered 2D crystals presented here are a first essential step towards this goal.

ACKNOWLEDGMENTS

We thank Deryck Mills for the introduction and expert support with the Jeol 3000SFF microscope and Vinzenz Unger for advice on the use of the MAKETRAN routine. We are indebted to Yoshinori Fujiyoshi, Kaoru Mitsuoka and Thomas Walz for providing the AQP1 data, Lorenz Hasler and Shirley Müller for their expert help. The work was supported by Swiss National Foundation for Scientific Research (NF grant No. 4036-44062 to AE), the M.E. Müller Foundation of Switzerland, and the National Institutes of Health (to PA).

REFERENCES

- Boos W Ehmann U Forkl H Klein W Rimmele M and Postma P 1990 Trehalose transport and metabolism in *Escherichia coli* *J Bacteriol* **172**: 3450-61
- Borgnia MJ Kozono D Calamita G Maloney PC and Agre P 1999 Functional reconstitution and characterization of AqpZ the *E coli* water channel protein *J Mol Biol* **291**: 1169-1179
- Cheng A van Hoek AN Yeager M Verkman AS and Mitra AK 1997 Three-dimensional organization of a human water channel *Nature* **387**: 627-630
- Froger A Tallur B Thomas D and Delamarche C 1998 Prediction of functional residues in water channels and related proteins *Protein Sci* **7**: 1458-1468
- Hasler L Walz T Tittmann P Gross H Kistler J and Engel A 1998 Purified lens major intrinsic protein MIP forms highly ordered tetragonal two-dimensional arrays by reconstitution *J Mol Biol* **279**: 855-864
- Henderson R Baldwin JM Ceska TA Zemlin F Beckmann E and Downing KH 1990 Model for the structure of *Bacteriorhodopsin* based on high-resolution electron cryo-microscopy *J Mol Biol* **213**: 899- 929
- Henderson R Baldwin JM Downing KH Lepault J and Zemlin F 1986 Structure of purple membrane from *Halobacterium halobium* : recording measurement and evaluation of electron micrographs at 35 Å resolution *Ultramicroscopy* **19**: 147-178
- Heymann B and Engel A 2000 Structural Clues in the Sequences of the Aquaporins *J Mol Biol* **295**: 1039-1053
- Jap BK Zulauf M Scheybani T Hefti A Baumeister W Aebi U and Engel A 1992 2D crystallization: from art to science *Ultramicroscopy* **46**: 45-84
- Jung JS Preston GM Smith BL Guggino WB and Agre P 1994 Molecular structure of the water channel through aquaporin CHIP The hourglass model *J Biol Chem* **269**: 14648-14654
- Lagree V Froger A Deschamps S Hubert JF Delamarche C Bonnet G Thomas D Gouranton J and Pellerin I 1999 Switch from an aquaporin to a glycerol channel by two amino acids substitution *J Biol Chem* **274**: 6817-6819
- Li H Lee S and Jap BK 1997 Molecular design of aquaporin-1 water channel as revealed by electron crystallography [letter] [see comments] *Nature Struct Biol* **4** 263-265
- Maurel C Reizer J Schroeder JI Chrispeels MJ and Saier MH Jr 1994 Functional characterization of the *Escherichia coli* glycerol facilitator GlpF in *Xenopus* oocytes *J Biol Chem* **269**: 11869-11872

- Mitsuoka K Murata K Walz T Hirai T Agre P Heymann JB Engel A and Fujiyoshi Y 1999 The Structure of Aquaporin-1 at 4.5-Å Resolution Reveals Short alpha-Helices in the Center of the Monomer *J Struct Biol* **128**: 34-43
- Mulders SM Preston GM Deen PM Guggino WB van Os CH and Agre P 1995 Water channel properties of major intrinsic protein of lens *J Biol Chem* **270**: 9010-9016
- Park JH and Saier MH Jr 1996 Phylogenetic characterization of the MIP family of transmembrane channel proteins *J Membr Biol* **153**: 171-180
- Reizer J Reizer A and Saier MH Jr 1993 The MIP family of integral membrane channel proteins: sequence comparisons evolutionary relationships reconstructed pathway of evolution and proposed functional differentiation of the two repeated halves of the proteins *Crit Rev Biochem Mol Biol* **28**: 235-257
- Ringler P Borgnia MJ Stahlberg H Maloney PC Agre P and Engel A 1999 Structure of the water channel AqpZ from *Escherichia coli* revealed by electron crystallography *J Mol Biol* **291**: 1181-1190
- Smith BL and Agre P 1991 Erythrocyte Mr 28000 transmembrane protein exists as a multisubunit oligomer similar to channel proteins *J Biol Chem* **266**: 6407-6415
- Voegele RT Sweet GD and Boos W 1993 Glycerol kinase of *Escherichia coli* is activated by interaction with the glycerol facilitator *J Bacteriol* **175**: 1087-1094
- Walz T Hirai T Murata K Heymann JB Mitsuoka K Fujiyoshi Y Smith BL Agre P and Engel A 1997 The three-dimensional structure of Aquaporin-1 *Nature* **387**: 624-627
- Walz T Smith BL Agre P and Engel A 1994 The three-dimensional structure of human erythrocyte aquaporin CHIP *EMBO J* **13**: 2985-2993